

Branched Copolymer Surfactants as Versatile Templates for Responsive Emulsifiers with Bespoke Temperature-Triggered Emulsion-Breaking or Gelation

Abhishek Rajbanshi, Marcelo Alves da Silva, Niamh Haslett, Philippa Cranwell, Neil Cunningham, Najet Mahmoudi, Darragh Murnane, Ewa Pavlova, Miroslav Slouf, Cecile Dreiss, and Michael Cook*

It has been found that the thermoresponsive behavior of emulsions stabilized by block copolymer surfactants (BCSs) can induce either gelation or emulsion break-up with mild temperature changes. A hydrophilic, steric-stabilizing component of the BCS, polyethylene glycol methacrylate (PEGMA), is crucial to control the thermoresponsive behavior of the emulsions: longer PEG chains (950 g mol^{-1}) lead to thermoregulation, whereas shorter PEGM chains (500 or 300 g mol^{-1}) lead to emulsion break-up upon mild heating. Additionally, the relative abundance of PEGMA to the thermoresponsive component in the BCS controls the gelation temperature of BCS-stabilized emulsions. Small-angle neutron scattering and transmission electron microscopy reveal that the BCS forms oblate ellipsoids which grow anisotropically with temperature. In samples that form a gel, there is evidence that these nano-objects form supra-colloidal structures, which are responsible for the gel mesophase formation. An optimal BCS can form emulsions that transition from a liquid to gel state when warmed above $32 \text{ }^\circ\text{C}$. This makes the system ideal for in situ gelation upon contact with the body. Overall, this study highlights the great potential of BCSs in generating thermoresponsive emulsions for drug delivery and other healthcare applications.

1. Introduction

“Engineered emulsions,” pioneered by Weaver and co-workers,^[1] are responsive emulsions stabilized by copolymer surfactants that switch from liquid to gel when triggered by an external stimulus. These materials were initially designed with pH-responsive behavior^[1,2] and have recently been further developed to exploit thermoresponsive properties.^[3,4] The gelation of the initial pH-responsive systems, based upon a poly(methacrylic acid) branched copolymer surfactant (BCS), was attributed to a droplet-assembly mechanism, whereby dispersed oil droplets interacted due to cooperative hydrogen bonding when carboxylate groups on the BCS switched to the corresponding carboxylic acid under acidic conditions.^[2,5] Thermoresponsive emulsions with temperature-induced viscosity

A. Rajbanshi, M. Alves da Silva, N. Haslett, D. Murnane, M. Cook
 School of Life and Medical Sciences
 University of Hertfordshire
 Hatfield, Hertfordshire AL10 9AB, UK
 E-mail: ucnv695@ucl.ac.uk


A. Rajbanshi, C. Dreiss
 Institute of Pharmaceutical Science
 King's College London
 London SE1 9NH, UK

P. Cranwell, N. Cunningham
 Centre for Industrial Rheology
 The Long Barn
 Warnford, Hampshire SO32 3LE, UK

N. Mahmoudi
 ISIS Neutron and Muon Source
 Rutherford Appleton Laboratory
 OX11 0QX Didcot, UK

E. Pavlova, M. Slouf
 Institute of Macromolecular Chemistry
 Czech Academy of Sciences
 Prague 16206, Czech Republic

M. Cook
 UCL School of Pharmacy
 University College London
 London WC1E 6BT, UK

 The ORCID identification number(s) for the author(s) of this article can be found under <https://doi.org/10.1002/admi.202300755>

© 2023 The Authors. Advanced Materials Interfaces published by Wiley-VCH GmbH. This is an open access article under the terms of the Creative Commons Attribution License, which permits use, distribution and reproduction in any medium, provided the original work is properly cited.

DOI: 10.1002/admi.202300755

changes were originally demonstrated by Koh and Saunders using graft copolymers of poly(*N*-isopropyl acrylamide) and poly(ethylene glycol) methacrylate (PEGMA), indicating that the concept of using temperature-responsive units in the polymer composition may achieve this phenomenon for BCS systems.^[6] Subsequent thermoresponsive BCS-stabilized emulsion systems exhibited complex gelation mechanisms, relying on polymer self-assembly in the bulk and concomitant network formation with BCS at the oil-water interface.^[3] Thus, polymer architecture effects are highly complex, affecting both the solution and interfacial behaviors that underpin the macroscopic phase changes. A particular elegance of this approach is that the BCS used may be synthesized in a highly scalable one-pot synthesis, routinely producing large (≈ 50 g) quantities of polymer without optimization.^[7] Furthermore, the feed mixture, containing components to induce stimuli-response, steric stabilization, branching, and hydrophobicity, contains many handles to precision-tune properties.^[8]

The liquid-gel transition enabled by stimuli-responsive BCS has particular application in areas such as drug delivery and cosmetics, where manipulation in a low viscosity state permits application to the body, after which the transition to a gel state allows retention and temporal stability,^[9,10] for example in prolonged drug delivery to the eye.^[11] There are, however, alternative stimuli-responsive behaviors that are desirable in emulsion systems, such as the induction of emulsion breaking. Stimulus-triggered emulsion coalescence and breaking have applications in fields such as chemically enhanced oil recovery, where reservoir rock is flooded with surfactant to extract oil that subsequently requires extraction through destabilization of the emulsion.^[12,13] Typically, these processes require additional chemical treatment or high temperatures adding to cost, both monetary and environmental.^[13]

Herein, the control of BCS architecture by a single factor, the pendant poly(ethylene glycol) (PEG) chain length, has been shown to dictate whether emulsions stabilized by the polymer exhibit thermoresponsive gelation or breaking. Furthermore, a second factor, the monomer ratio, offers control over the liquid-gel transition temperature, allowing the bespoke generation of emulsions that respond to body temperature for *in situ* gelation to occur. The mechanisms dictating these behaviors have been explored using small-angle neutron scattering (SANS) and pendant drop tensiometry to elucidate nanoscale and interfacial behaviors in the system, where hierarchical assembly processes from the polymer to droplet level underpin thermoresponse.

2. Results and Discussion

Thermoresponsive BCSs can be synthesized by azobisisobutyronitrile (AIBN)-mediated free radical polymerization of a feed mixture containing diethylene glycol methyl ether methacrylate (DEGMA), PEGMA, ethylene glycol dimethacrylate (EGDMA) and dodecanethiol (DDT). In the resultant materials, DEGMA is thermoresponsive, exhibiting a lower critical solution temperature (LCST), PEGMA is hydrophilic, EGDMA induces branching, and DDT imparts dodecyl (C-12) chain ends to the BCS. A library of BCSs was synthesized to probe structure-function relationships imparted by the length and relative abundance of the PEGMA component (Table 1, Figure 1i). In principle, this

Table 1. Feed composition for the synthesis of BCS1-6.

Sample ID:	BCS1	BCS2	BCS3	BC4	BCS5	BCS6
PEGMA-950 (mmol)	6	–	–	4.5	3	1.5
PEGMA-500 (mmol)	–	6	–	–	–	–
PEGMA-300 (mmol)	–	–	6	–	–	–
DEGMA (mmol)	174	174	174	174	174	174
EGDMA (mmol)	12	12	12	12	12	12
DDT (mmol)	12	12	12	12	12	12
AIBN (mmol)	1.2	1.2	1.2	1.2	1.2	1.2

component serves several functions: crucially, PEGMA can allow steric stabilization of the oil-water interface in emulsion systems;^[1] furthermore, its abundance potentially mediates transition temperatures, as observed in linear polymer systems.^[14,15] Two series of BCS were successfully synthesized and characterized by ¹H NMR spectroscopy (Figure 1ii) and gel-permeation chromatography (GPC) (Figure 1iii, Table S1, Supporting Information). The purity of all polymers was >99% by ¹H NMR, and GPC traces showed that the polymer molecular weight distribution was monomodal. M_n was impacted in the samples by the 12–14 kDa membrane used for purification by dialysis. However, this purification method was previously found to be necessary for the BCS to exhibit thermogelation.^[3] The first series evaluated the effect of PEG M_n within the PEGMA component, with BCS1 to 3 progressively reducing the length of these pendant PEG chains from 950 to 500 to 300 g mol⁻¹ M_n PEGMA, having 19–20, 9–10, and 4–5 ethylene oxide units, respectively (Figure 1iv, with full composition in methods, Table 1). The hydrophilicity and LCST in the aqueous solution of PEGMA analogs increase with an increase in molecular weight of the macromonomer.^[16] However, these PEGMA components exhibit LCST in aqueous solution between 60 °C to 90 °C as homopolymers, beyond the temperature range studied and thus are intended to be hydrophilic in the study.^[14,17,18] The second series evaluated the effect of the PEGMA abundance, with BCS1 through BCS4-6 containing serial reduction in PEGMA feed concentration of 6, 4.5, 3, and 1.5 mmol, respectively (Figure 1iv). In both series, the feed ratio of thermoresponsive macromonomer (DEGMA), crosslinker (EGDMA), initiator (AIBN), and chain transfer agent (DDT) were kept constant. The effect of the systematic variation in structure in the BCS series is diagrammatically shown in Figure 1iv.

Emulsions were prepared by homogenization of equal mass of dodecane and BCS solution in water at 2.5–10 wt.% BCS relative to the total mass of the system. The resulting oil-in-water emulsion exhibited creaming over 36 h and the lower water phase was removed to yield concentrated emulsions (the final volume fraction of oil was $\varphi_{oil} = 0.72$). When heating the samples and observing their appearance by eye, two distinct thermoresponsive behaviors were observed depending on BCS architecture. Reducing the PEGMA chain length to 500 (BCS2) and 300 g mol⁻¹ (BCS3) gave emulsions with temperature-induced breaking (e.g., BCS3, Figure 2i), whilst the 950 molecular weight gave thermoreversible gelation (e.g., BCS5, Figure 2i). Both phenomena have exciting potential in the design of advanced functional materials, and control over which behavior is exhibited was enabled by a single factor; the length of PEG chains dangling from the

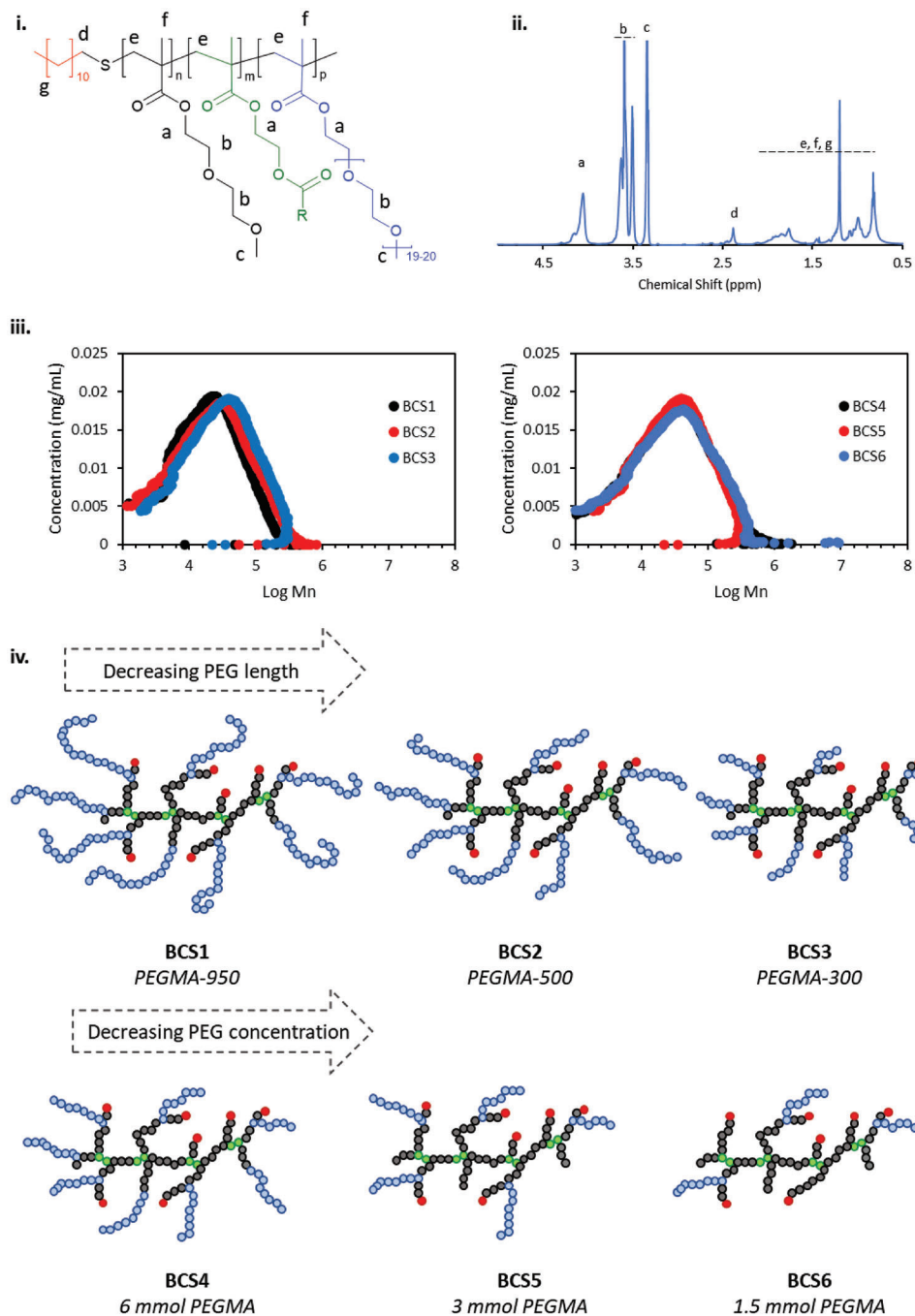


Figure 1. Schematic representation of the chemical structure of DEGMA BCS i) on which a polymer library is based and exemplar ¹H NMR spectrum of BCS1 ii). GPC chromatograms for the six BCS systems iii). The factors investigated in the library, color-coded against the chemical structure i), are shown diagrammatically iv), and contained in full in Table 1.

BCS structure. The thermoresponsive breaking of emulsions was explored by hot-stage microscopy. BCS3 emulsions were subjected to a temperature ramp from 5 to 30 °C at 1 °C min⁻¹ and micrographs were recorded (Figure 2ii). Droplets were unaffected by temperature between 5 and 20 °C, with droplet diameters between 4 and 53 μm. However, upon heating the BCS3 emulsion to between 25 and 30 °C, rapid droplet coalescence was observed. 20 wt.% aqueous solutions of BCS1, BCS2, and BCS3

demonstrated distinct behaviors on heating, with BCS1 increasing in viscosity at 39 °C, but BCS 2 and 3 undergoing phase separation from 24 and 22 °C, respectively. Further evaluation of all BCS emulsion systems was conducted using rheology to explore the materials in more detail.

The rheological evaluation of the 1:1 oil-in-water emulsion system stabilized by varying concentrations of BCS was performed by small-amplitude oscillatory shear temperature ramps

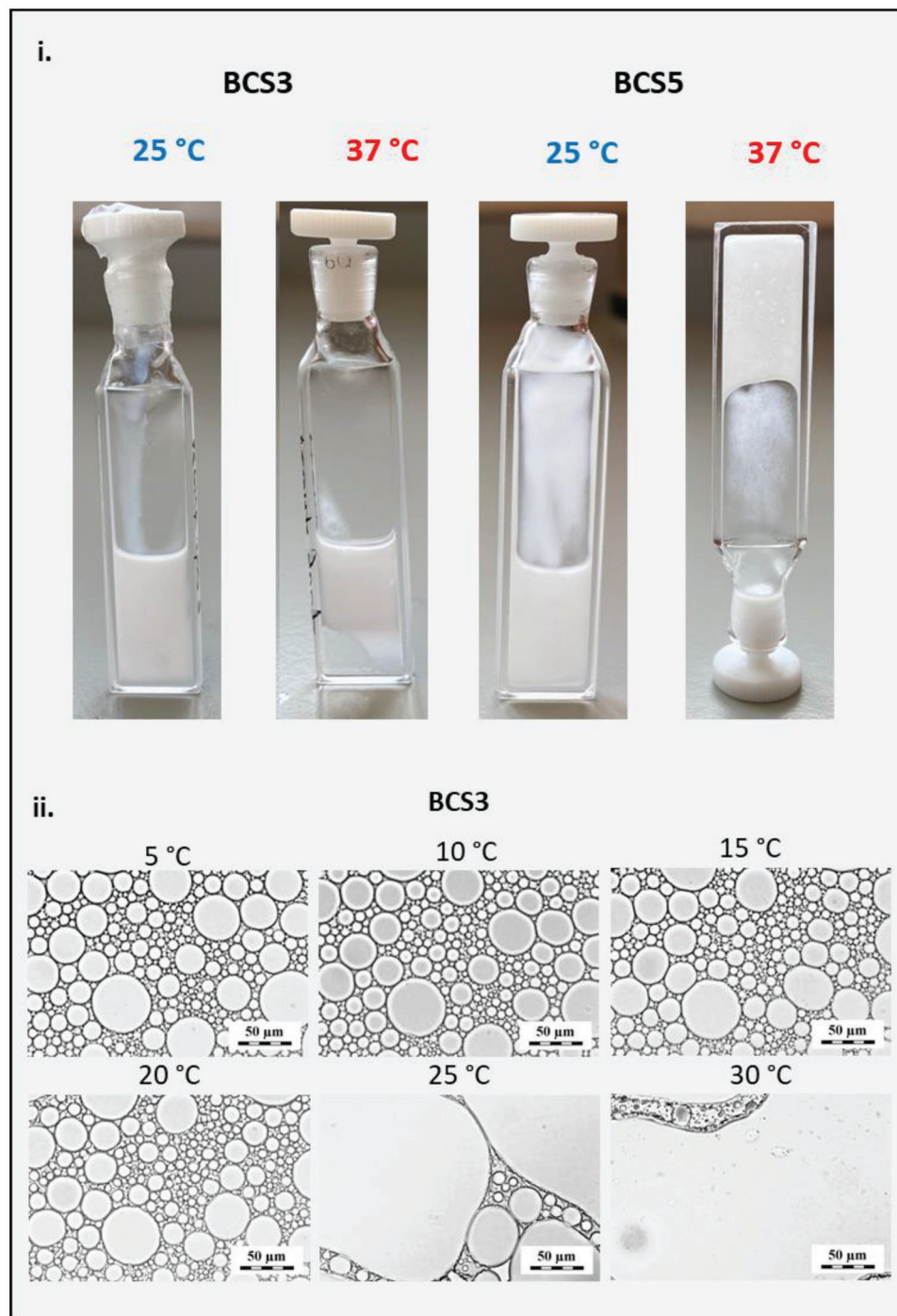


Figure 2. BCS-stabilized emulsions can exhibit either temperature-induced breaking or gelation at physiologically relevant temperatures. Emulsions shown are stabilized by 10 wt.% BCS and displayed macroscopic phase changes i). Microscopic evaluation at 20 x magnification demonstrates fast coalescence in the BCS3 system at $T > 20$ °C ii).

(Figure 3). The rheology data demonstrate the dependence of the storage, (G') and loss, (G'') moduli with temperature at a fixed, small stress amplitude (1 Pa) and angular frequency (6.283 rad s^{-1}). BCS concentration showed a strong influence on thermoresponsive activity, which could be manipulated to trigger thermo-gelation. BCS1 is the reference system, representing

the emulsions stabilized by the BCS synthesized with PEGMA-950. At 2.5 wt.% and 5 wt.% polymer concentrations, emulsion G' and G'' increased with the influence of temperature at 45 °C but a gel did not form. However, at 10 wt.% polymer concentration, a significant rise in G' and G'' is observed, leading to gelation at 48 °C (defined here by the G' cross over G'' point).^[19] The

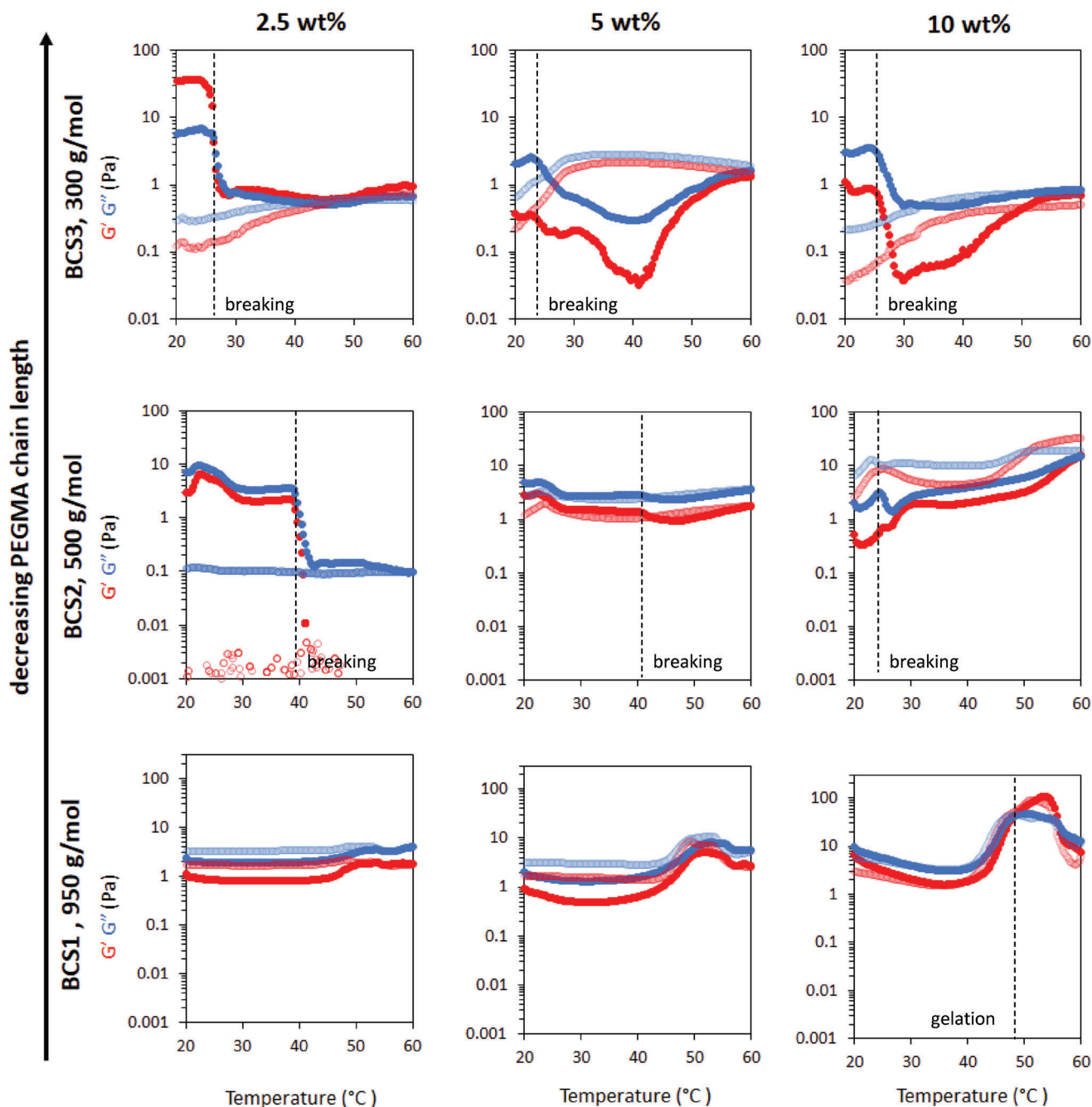


Figure 3. Rheological behavior of emulsions stabilized by thermoresponsive BCS1-3, probing the effect of PEGMA chain length. Emulsions were explored at 2.5, 5, and 10 wt.% polymer concentrations. G' is shown in red and G'' is shown in blue. Dark colors show the “up” ramp whilst light colors show the subsequent “down” ramp.

process was then reversed on the cooling cycle. Emulsions stabilized with BCS2 (i.e., BCS copolymerized with PEGMA-500 instead of PEGMA-950) demonstrated a contrasting response to temperature. At 2.5 wt.%, a slight rise in G' and G'' was observed initially, which was not stable, leading to emulsion thinning at ≈ 23 °C and eventually the breaking of the emulsion at 40 °C, appearing as a sharp reduction in G' and G'' . A similar behavior was observed for the emulsion stabilized at 5 wt.% BCS, with slight thickening at the start of the tem-

perature ramp, leading to thinning at 23 °C and emulsion break-up at 40 °C, which was confirmed by visual observation of the system. At 10 wt.% polymer concentration, emulsion breaking was observed visually with a rise in temperature at ≈ 25 °C. The emulsion stabilized with BCS3 (i.e., BCS copolymerized with PEGMA300) also demonstrated emulsion thinning, with response to temperature eventually leading to emulsion breaking. Emulsion breaking was observed at 25 °C at all BCS3 concentrations of 2.5, 5, and 10 wt.%. Rheological

events after emulsion breaking are not discussed due to the complexity of the biphasic system. It can also be seen across the series that the thermal events move to lower temperatures as the PEGMA M_n is reduced, likely related to a reduced LCST as the hydrophilicity of the polymer is reduced, typical for thermoresponsive systems.^[20,21]

This study of the rheological behavior of emulsions stabilized by BCS1-3 suggested that emulsion thickening or thermogelation, and emulsion thinning or even emulsion breaking, could be controlled by varying the chain length of PEGMA. This may be due to the PEGMA moiety offering steric stabilization to the emulsion after the BCS tethers to the oil-water interface.^[1] Thus, when DEGMA switches to a relatively hydrophobic state above the LCST, the PEGMA is hypothesized to offer sufficient steric stabilization to halt coalescence events. Thus, it is likely that the reduced chain length of the PEG chains adorning the BCS reduces the ability to stabilize the emulsion when DEGMA is hydrophobic above the LCST. An additional factor is that the hydrophilicity of PEGMA increases with an increase in molecular weight and the thermoresponsive behavior is related to the amphiphilic character of these macromolecules.^[22] This factor most likely impacts transition temperatures by reducing the LCST with lower PEGMA chain lengths, particularly evident in the 2.5 wt.% emulsions. Overall, these thermoresponsive BCSs can be widely employed due to their ability to switch thermoresponsive behavior. This approach of synthesizing thermoreversible gels can be used, for example, in the healthcare sector to develop drug delivery platforms with in situ gelation combined with the capacity to solubilize hydrophobic molecules. However, with the current systems, the gelation temperatures are not physiologically relevant.

The LCST of oligoethylene glycol methacrylate is dependent upon the degree of polymerization of the macromonomer.^[14] It is known that in copolymers of oligoethylene glycol methacrylates with different chain lengths, the LCST may be tuned with a tendency toward the LCST expected from the constituent monomer of greatest abundance.^[23] Thus, it was anticipated that increasing the relative abundance of DEGMA would show a trend toward the LCST of poly(DEGMA), $\approx 26^\circ\text{C}$.^[23,24] Adapting this concept, analogs of BCS1 were synthesized with a varying molar feed ratio of PEGMA-950. BCS1 was synthesized with 6 mmol of PEGMA-950 whereas BCS4, BCS5, and BCS6 were synthesized with 4.5, 3, and 1.5 mmol of PEGMA-950 keeping the feed ratio of DEGMA, EGDMA, and 1-DDT constant. 20 wt.% aqueous solutions of BCS1, BCS4, and BCS5 were turbid at room temperature, but exhibited an increase in viscosity by vial inversion studies at 39, 38, and 38 $^\circ\text{C}$, respectively, whereas BCS6 did not exhibit any visual evidence of viscosity changes in the range 20–50 $^\circ\text{C}$.

Figure 4 shows the rheology of thermoresponsive emulsions stabilized with BCS1,4-6 (decreasing the molar feed ratio of PEGMA-950, Figure 1iv, Table 1) at BCS concentrations of 2.5, 5, and 10 wt.%. The emulsion systems stabilized at 2.5 wt.% concentration of BCS1,4-6 demonstrated a slight rise in G' and G'' indicating thermothickening behavior. It is observed that the temperature at which the emulsion showed thickening decreased from ≈ 45 to 30 $^\circ\text{C}$ with a decrease in the molar ratio of PEGMA-950. Similar rheological behavior was observed for emulsions stabilized at 5 wt.%, with the thickening temperature declining with a decrease in PEGMA-950 molar concentration. The emulsion remained predominantly liquid-like, and gelation did not occur ($G' < G''$).

For the emulsion system stabilized with BCS1 at 10 wt.% concentration, thermogelation ($G' > G''$) was observed at 48 $^\circ\text{C}$, which was reversed on the cooling cycle. Similarly, reversible thermogelation occurred at 40, 35, and 26 $^\circ\text{C}$ for emulsions stabilized by BCS4, BCS5, and BCS6 at 10 wt.% concentration. In the BCS6 system this gelation is particularly subtle, but does meet the criterion $G' > G''$. It is believed that these thermal transitions relate to the LCST transition of the BCS series as typical for copolymer systems,^[18,25–27] showing a reduced LCST as the relative fraction of DEGMA is increased, in line with the observation that in mixed OEGMA systems, the LCST tends toward that of the most abundant monomer.^[23] Overall, this study demonstrates that the gelation temperature of thermoresponsive engineered emulsion stabilized by BCSs can be controlled by varying the mole ratio of PEGMA-950 during synthesis. This design principle can generate advanced functional materials allowing the tuning of thermoresponsive engineered emulsions to gel at physiological temperature for applications including drug delivery to topical sites or depot injections.^[28]

Next, pendant drop tensiometry was used to probe the effects of BCS characteristics and temperature on surface tension, as little information is known about DEGMA BCS behavior at interfaces (**Figure 5**). BCS3 and BCS5 were selected as two representative systems where BCS3 leads to emulsions that break with temperature, and BCS5 leads to emulsions with thermoreversible gelation. Both BCS reduced the surface tension of water substantially (from 72 to 43–45 mN m^{-1} at 25 $^\circ\text{C}$), evidencing their ability to adsorb to this interface, similar to observations for N-isopropylacrylamide BCS.^[3] Heating the system from 20 to 37 $^\circ\text{C}$ led to a small increase in surface tension in solutions for both BCSs measured, which was still lower than the surface tension of water. A time study indicated that the surface tension was stable over a period of 5 min in both systems and at both temperatures but with some evidence of drift to higher surface tension in the BCS5 system at 37 $^\circ\text{C}$ with time. However, this was at longer timescales than that required for emulsion breaking (Figure 5iii).

The authors suggest that the difference between emulsion breaking (BCS3) and emulsion stability (BCS5) when heated is due to steric effects from the PEGMA component. This is included in the BCS structure to sterically stabilize the emulsion droplets, as it is expected that over the temperature range studied PEG is highly hydrophilic and will extend into the water phase, providing a steric barrier to coalescence.^[8,29] BCS3 and BCS5 contain PEGMA with molecular weight 300 and 950 g mol^{-1} , respectively. The reduced degree of polymerization of the PEGMA component in BCS3 may mean that once DEGMA is above its LCST, there is insufficient steric stabilization of the droplets. In BCS5, the degree of polymerization of PEGMA is greater, leading to stability even above the LCST.

SANS was employed to probe the nanostructure of the BCS solutions in D_2O (**Figure 6**). The BCS architecture has previously been reported to give oblate ellipsoidal particles, particularly above the LCST of DEGMA. Data fitting was conducted using an ellipsoidal form factor to account for scattering in BCS solutions. The volume fraction of the scattering objects was initially assumed to be equivalent to the weight fraction due to the similar density of the BCS constituents (PEG density: 1.125 g mL^{-1}) and D_2O (density: 1.11 g mL^{-1}), and only altered when a satisfactory fit could otherwise not be obtained. The scattering length

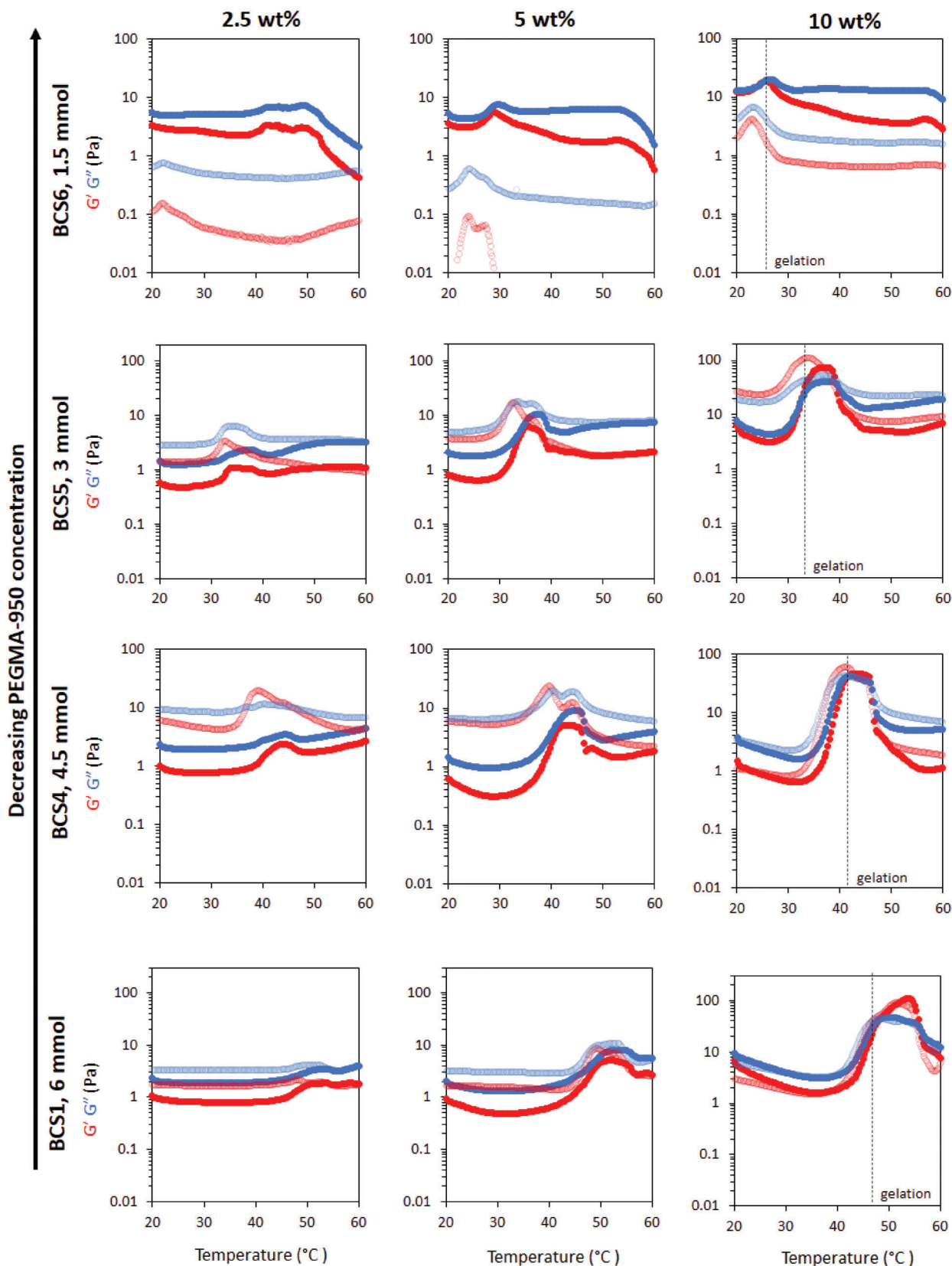


Figure 4. Effect of PEGMA-950 concentration on the gelation temperature of thermoresponsive engineered emulsions. Emulsions were stabilized by BCSs with BCS1 synthesized with 6 mmol, BCS4 with 4.5 mmol, BCS5 with 3 mmol, and BCS6 with 1.5 mmol of PEGMA-950.

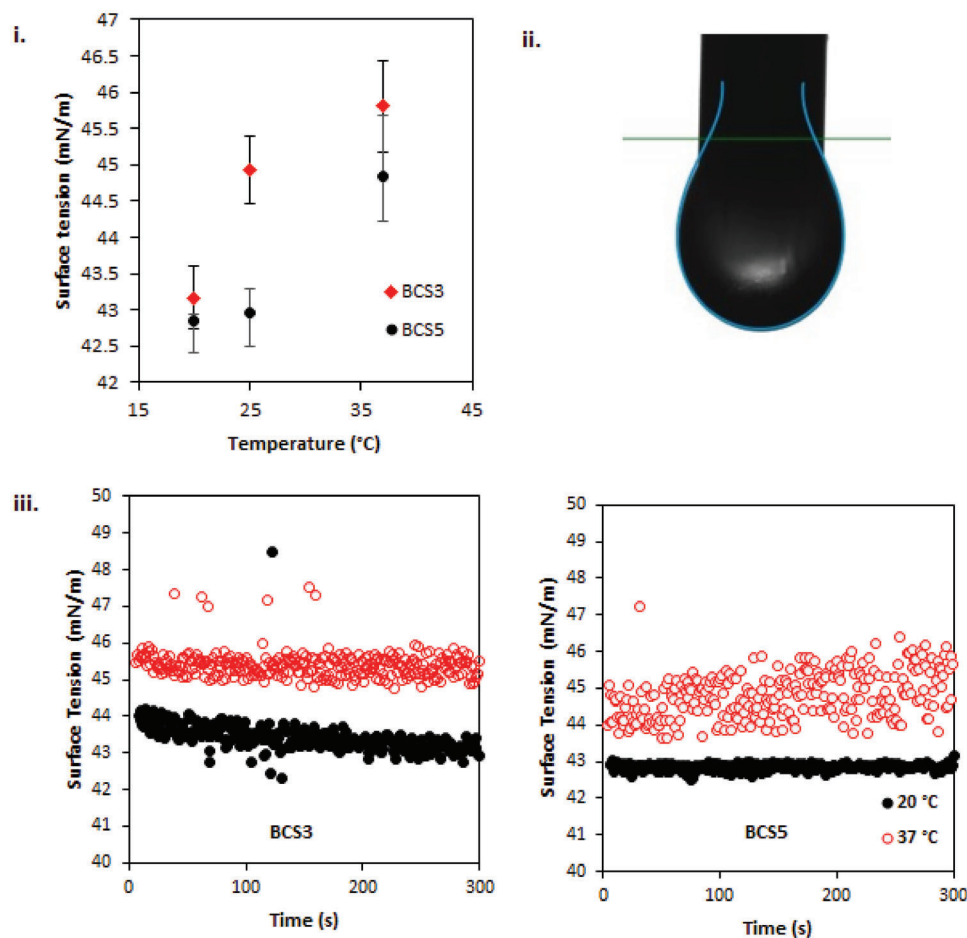


Figure 5. Pendant drop tensiometry of BCS3 and BCS5 aqueous solutions (20 wt.%) with the variation of temperature. Surface tension measurements were conducted i) with fitting using the Owens, Wendt, Rabel, and Kaelble method ii). Time-dependence of surface tension is also shown iii).

density of D₂O is known ($6.37 \times 10^{-6} \text{ \AA}^{-2}$), and the SLD of the BCS components may be calculated (e.g., DDT: $-0.368 \times 10^{-6} \text{ \AA}^{-2}$, DEGMA: $0.471 \times 10^{-6} \text{ \AA}^{-2}$),^[30] however it is expected that the aggregates remain solvated to some degree by D₂O even above the LCST^[31] so the scattering length density was fitted (and not fixed). The ellipsoidal form factor gave satisfactory fits to the intermediate and high q region ($\approx 0.01 < q < 0.3 \text{ \AA}^{-1}$), but in some instances, a power law was required to fit the low q region ($\approx 0.01 \text{ \AA}^{-1} > q$). In all cases, this power law took the form $I(q) = q^{-4}$, consistent with Porod-type scattering from larger aggregates with a sharp interface. The exact nature of these aggregates cannot be determined, and discussion about their nature is limited.

Reducing PEGMA chain length demonstrated a switch from thermogelation (BCS1) to temperature-responsive demulsification (BCS2-3). SANS was used to probe the solution and emulsion behavior of the PEGMA-500 and PEGMA-300 systems, designated BCS2 and BCS3, respectively, at temperatures below their macroscopic phase separation (Figure 6, Tables S2 and S3, Supporting Information). The emulsion of BCS1 with PEGMA-950 was also measured by SANS as a reference, where solution behavior is already known.^[4] Fitting BCS2 solutions to an ellipsoid

form factor gave spheres (i.e., equatorial = polar radius) of radius 32 Å at 15 °C, but transitioned into an ellipsoid at 25 °C (equatorial radius/polar radius = 4.34). This ellipsoid was oblate with an equatorial radius of 98 Å and a polar radius of 22 Å, in line with prior studies of BCS systems.^[4] The spherical form at 15 °C is the expected thermodynamically favorable colloidal structure to assume, however deviation from this, as observed at 25 °C, is possible due to steric constraints in the polymer. It is known that these BCSs exhibit a CAC (critical aggregation concentration),^[3] thus it is believed that the nano-objects at low temperatures are formed by the assembly of multiple BCSs via hydrophobic interaction of the polymer terminus. Upon heating to 25 °C, some degree of conformation change may occur in the BCS due to desolvation of the LCST-exhibiting DEGMA component. This, in turn, reduces the effective hydrophilic head group volume of the polymeric surfactant, leading to a transition to oblate ellipsoids, as described by the critical packing parameter theory, which holds for block copolymers.^[32] In a similar manner, BCS3 forms oblate ellipsoidal aggregates at 15 °C, which may also be understood as a reduction in hydrophilic head group volume when the PEGMA-500 component of BCS2 is reduced to PEGMA-300 in BCS3. This ellipsoidal geometry is observable by TEM (Figure 6) when BCS3

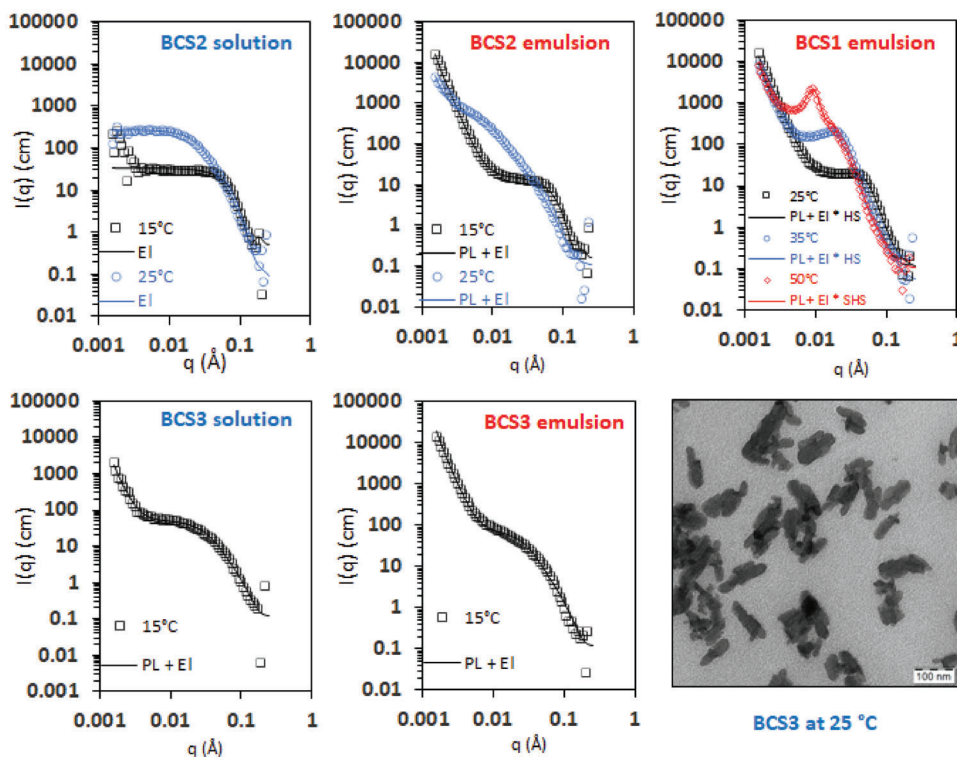


Figure 6. SANS of BCS2/3 solutions (20 wt.%) in D_2O and BCS1-3 (10 wt.%) d-dodecane/ D_2O emulsions. Data were presented at 25, 35, and 45 °C in black, blue, and red symbols, respectively. Fits to data are shown as continuous lines, with the models used displayed in the legend. EI is an ellipsoid, PL is a power law, and SHS is the sticky-hard-sphere structure factor. A TEM image of BCS3 is included at 25 °C.

is heated above the point of emulsion breaking, 25 °C. Sizing these particles in ImageJ gave dimensions of $69 \pm 13 \times 26 \pm 6$ nm ($n = 5$), with an equatorial/polar ratio of 2.6. Despite differences in sample preparation method, TEM provides further proof of the existence of these ellipsoidal nano-objects.

In emulsion systems of BCS2 and BCS3, the spherical/ellipsoidal structures remain observable in the SANS profiles, however with a marked q^{-4} decay at low q . This is believed to arise from the interface of the larger d-dodecane droplets. Above 25 and 15 °C for BCS2 and BCS3, respectively, the BCS solutions/emulsions underwent macroscopic phase separation and SANS measurements were not conducted. The BCS1 emulsion, which displays thermogelation, exhibited features not seen in the BCS2/BCS3 systems. Again, oblate ellipsoidal nano-objects are present with Porod-type behavior at low q . The ellipsoidal objects grew anisotropically, from 28×61 Å at 25 °C to 67×350 Å at 50 °C (polar \times equatorial radii). This effect is attributed to further desolvation of the DEGMA component reducing headgroup size as heating increases. The BCS1 emulsion also requires a structure factor to fit the data adequately, indicating the presence of strong interactions between the colloidal assemblies. At low temperatures, a fit to a hard-sphere structure factor indicates that the objects interact via hard-sphere interactions without interpenetration. Instead, at 50 °C, where the emulsions are in the gel state, a sticky hard sphere structure factor was required to fit the very marked peak at $q = 9.16 \times 10^{-3} \text{ \AA}^{-1}$. This indicates the presence of an attractive well and interactions between the BCS aggregates, giving information that the gel

state occurring under this condition is underpinned by supra-colloidal aggregates of oblate ellipsoids formed by multiple BCSs.

The BCS4-6 series was then examined by SANS (Figure 7, Tables S4 and S5, Supporting Information), which explores a reduction in PEGMA concentration in the feed mixture, from 6 mmol in BCS1 to 4.5, 3, and 1.5 mmol, in BCS4, 5 and 6, respectively. All these emulsions exhibited thermothickening behavior, as measured by rheology, with the temperature at which an increase in G' and G'' was observed decreasing with the PEGMA content of the BCS. SANS was conducted on BCS solutions at 25, 35, and 45 °C to compare the systems that allowed emulsions to switch between liquid and gel states. At 25 °C, BCS4-6 solutions contained oblate ellipsoidal nano-objects with a Porod character at low q , assigned to clustering of the polymer.^[33] Upon heating, the ellipsoids increased in size and had an increasing oblate character, with the ratio of equatorial to polar radius increasing (Figure 8). BCS4 required a hard sphere structure factor for fitting, whereas BCS5 required a sticky-hard-sphere structure factor to fit the data, as did BCS6. The BCS6 phase separated at high temperatures, hence the data at 45 °C are omitted. The lack of attractive interactions in BCS4, which did not require a sticky-hard-sphere structure factor, is attributed to the temperature at which the SANS was conducted. The corresponding emulsion is in a liquid state at 25 and 35 °C and transitions into a gel between 42 and 45 °C. The measurement is therefore taken at a transition temperature where the elastic character starts to reduce. BCS5, which exhibited gelation at the most appropriate temperature for

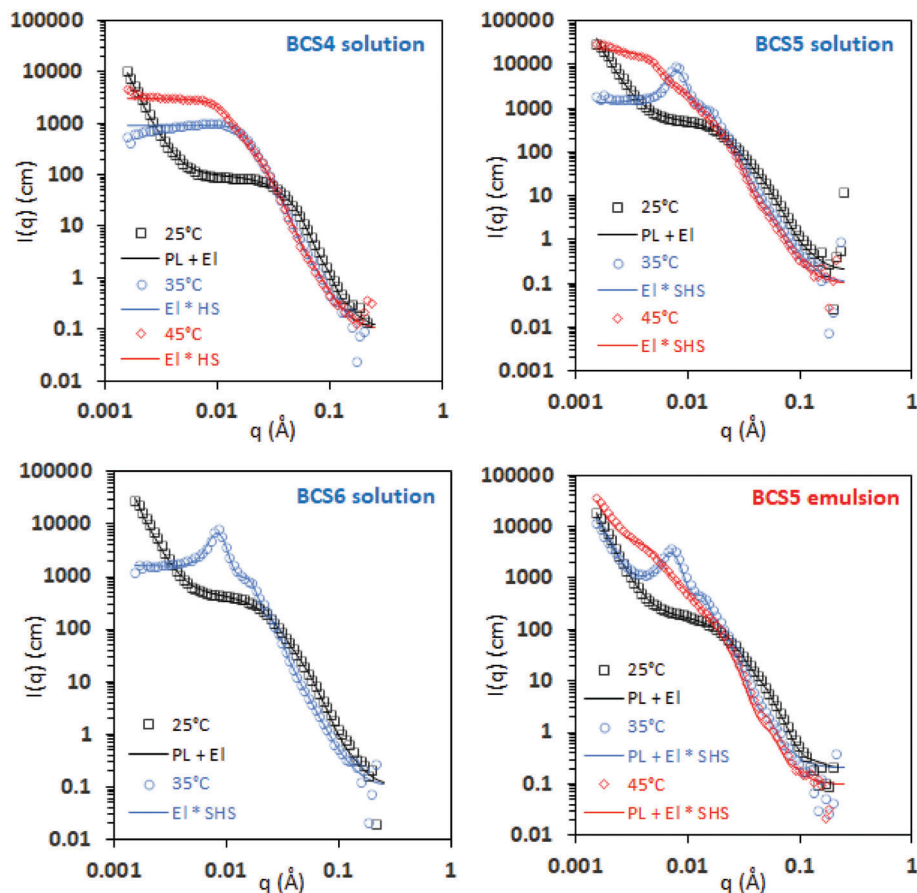


Figure 7. SANS of BCS4-6 solutions (20 wt.%) in D₂O and BCS5 (10 wt.%) d-dodecane/D₂O emulsion. Data were presented at 25, 35, and 45 °C in black, blue, and red symbols, respectively. Fits data are shown in the continuous lines, with the models used shown in the legend. EI is an ellipsoid, PL is a power law, and SHS is the sticky-hard-sphere structure factor.

healthcare applications (32 °C), was also studied by SANS in an emulsion system (Figure 7). The oblate ellipsoidal particles were retained and exhibited comparable transitions to the solution system, giving evidence that the solution behavior reported thus far is retained in the emulsion system. A pronounced upturn at low q was also present, associated with the interface of the emulsion droplets.

3. Conclusions

The BCS architecture is highly versatile in generating thermoresponsive emulsions with either reversible gelation or emulsion breaking, even with mild temperature changes. The PEG component of BCS is crucial to control the thermoresponsive behavior of the emulsions. With longer PEG lengths

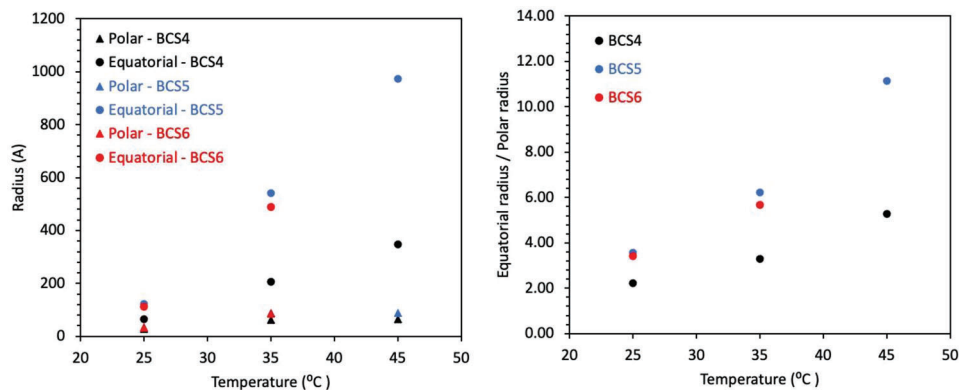


Figure 8. Fitting parameters extracted from the ellipsoidal form factor used in the analysis of BCS2-4 solutions.

(950 g mol⁻¹), the emulsions exhibit thermogelation, whereas shorter PEG chains (500 or 300 g mol⁻¹) lead to emulsion breaking upon mild warming. This is attributed to reduced steric stabilization of the droplets above the LCST of DEGMA by the hydrophilic PEG chains with reduced length. The relative abundance of PEGMA in the BCS tightly controls the gelation temperature of BCS-stabilized emulsions. Decreasing the concentration of PEGMA leads to a reduction in the temperature at which gelation occurs. SANS reveals that the BCSs formed oblate ellipsoids in both solution and emulsion systems, which grew anisotropically with temperature. In samples that formed a gel, there was evidence that these nano-objects formed supra-colloidal structures, which would be responsible for gelation. An optimal BCS architecture, BCS5, can form emulsions that transition from a liquid to a gel state when warmed above 32 °C, making this system ideal for in situ gelation upon contact with the body. This material has great potential in healthcare applications, where responsive behavior can be paired with an emulsion system, enabling the solubilization of a wide range of drug chemistries.

4. Experimental Section

Material: Di(ethylene glycol) methyl ether methacrylate (DEGMA, 95%), poly(ethylene glycol) methyl ether methacrylate (PEGMA-950, Mn 950 g mol⁻¹), poly(ethylene glycol) methyl ether methacrylate (PEGMA-500, Mn 500 g mol⁻¹), poly(ethylene glycol) methyl ether methacrylate (PEGMA-300, Mn 300 g mol⁻¹), ethylene glycol dimethacrylate (EGDMA, 98%, Mn 198 g mol⁻¹), 1-dodecanethiol (DDT, 99%), and anhydrous dodecane (99%) were purchased from Sigma-Aldrich (UK). Dodecane-d26 was purchased from QMX (UK). α , α -Azobisisobutyronitrile (AIBN, >99%) was obtained from Molekula (UK). Absolute ethanol was supplied by VWR (UK). Dialysis tubing with molecular weight cut-off (MWCO) of 12–14 kDa was purchased from Sigma Aldrich (UK). Deionized H₂O was employed in all experiments. All chemicals were used as received.

Synthesis of Branched Copolymer Surfactant by Free Radical Polymerisation: Thermoresponsive BCS comprising DEGMA, PEGMA-950/PEGMA-500/PEGMA-300, EGDMA, and DDT (Table 1) were prepared following the synthesis procedure described previously.^[4] Six polymers were synthesized, labeled as BCS1-6, using DEGMA as an LCST-imparting thermoresponsive monomer (Table 1). BCS1-3 was synthesized with varying chain lengths of PEGMA functioning as a non-LCST hydrophilic macromonomer for BCS stabilization. BCS1 was synthesized with PEGMA-950, BCS2 was stabilized by replacing PEGMA-950 with PEGMA-500 and BCS3 with PEGMA-300. BCS4-6 reduced the quantity of PEGMA-950 in the feed from 6 (BCS1) to 1.5 (BCS6).

In a general synthesis, DEGMA, PEGMA, EGDMA, and DDT (quantities in Table 1) were dissolved in ethanol (190 mL) and sparged with nitrogen gas for 1 h. A solution of AIBN (190 mg) in ethanol (10 mL), also sparged with nitrogen gas for 1 h, was then added to the solution. The reaction was heated to 70 °C for polymerization to proceed and stirred continuously. After 48 h, the reaction mixture was subjected to distillation to remove excess ethanol. The resultant crude polymer was dissolved in water and transferred to a presoaked dialysis bag. The dialysis bag was immersed in deionized water for 7–10 days and the water was replaced at regular intervals to facilitate the purification process. The resultant polymer solution was subjected to lyophilization for 48 h to obtain a freeze-dried product. Yield: 85 ± 1%. An initial study of phase behavior was conducted by preparing 20 wt.% aqueous solutions of each BCS and heating in a water bath at 1 °C increments between 15 and 50 °C. An equilibration time of 5 min was employed before visual observation.

Characterization of Thermoresponsive BCSs: ¹H NMR spectroscopy was used to characterize the BCS using a Bruker Advance AM 600 NMR instrument. All samples were prepared in CDCl₃, using the residual solvent peak as an internal standard.

Gel-permeation chromatography was conducted using an Agilent Infinity II MDS instrument equipped with differential refractive index, viscometry, dual-angle light scatter, and variable wavelength UV detectors. The system was equipped with 2 x PLgel Mixed D columns (300 × 7.5 mm) and a PLgel 5 μ m guard column. The eluent was DMF with 5 mmol NH₄BF₄ additive. Samples were run at 1 mL min⁻¹ at 50 °C. Poly(methyl methacrylate) standards (Agilent EasiVials) were used for conventional and universal calibration between 955 000 and 550 g mol⁻¹. Analyte samples were filtered through a nylon membrane with 0.22 μ m pore size before injection. Number-average molar mass (Mn) and dispersity (\bar{M}_w/\bar{M}_n) values were determined by universal calibration using Agilent GPC/SEC software.

Preparation of Water-in-Oil Emulsion Stabilized by BCS: A series of 1:1 w/w oil-in-water emulsions were prepared to study the thermoresponsive behavior by rheology. Aqueous polymer solution (2.5 g) at concentration levels of 5, 10 and 20 wt.% (2.5, 5, was prepared in ice-cold water in a 30 mL glass vial and left overnight in the refrigerator (\approx 4 °C) to solubilize. This was followed by the addition of dodecane oil phase (2.5 g) and the solution emulsified at 2400 rpm for 2 min using a Silverson L4R Heavy Duty Mixer Emulsifier (USA). The emulsions were left on the bench top to rest for 36 h at room temperature. Approximately 1.1 g of the water phase separated as the lower phase of the creamed emulsion and was withdrawn; the emulsion cream was studied in further experiments. Where quoted, the oil phase volume (φ_{oil}) was calculated by:

$$\varphi_{oil} = \frac{\left(\frac{2.5}{\rho_{oil}}\right)}{\left(\frac{2.5}{\rho_{oil}}\right) + (2.5 - \text{Mass Water})} \quad (1)$$

where “Mass Water” is the mass of the lower phase extracted after creaming. ρ_{oil} is the density of the oil (in that case 0.75 g mL⁻¹) and 2.5 is an individual mass of the oil and water added.

Rheology and Tensiometry of Thermoresponsive Emulsions: Rheology experiments were performed on an AR 1500ex rheometer by TA instruments (USA) equipped with a Peltier temperature control unit and a 40 mm parallel plate geometry with a specified gap distance of 500–750 μ m. Each emulsion’s creamed layer was placed on the rheometer lower plate prior to the measurement, after which temperature ramps were performed. Three minutes of equilibration at the desired temperature was conducted prior to measurement. Temperature ramps were performed in the range 20–60 °C, at 1 °C per minute heating rate, an oscillating stress of 1 Pa, and a frequency of 6.28 rad s⁻¹. The change in storage modulus (G') and loss modulus (G'') as a function of temperature was recorded.

Pendant drop analysis was undertaken using a Krüss DSA 100 Drop Shape Analyzer system. Measurements were taken at 19, 25, and 37 °C, with the sample open to the atmosphere. The polymer system under study was loaded into a syringe and then liquid was extruded in 2 μ L increments until the trigger line was exceeded (\approx 15 μ L). At this point, the droplet was held for 300 sec and the surface tension was continually monitored. An average surface tension was then calculated.

SANS of BCS Solutions and Emulsions: SANS experiments were conducted on the time-of-flight diffractometer instrument SANS2d at the STFC ISIS Neutron and Muon Source (UK). Incident wavelengths from 1.75 to 12.5 Å were used at a sample-to-detector distance of 12 m, which gave a scattering vector (q) range from 1.6×10^{-3} to 0.25 \AA^{-1} . The temperature of the samples was controlled by an external circulating water bath (Julabo, DE). Samples were loaded in 1 cm wide rectangular quartz cells with 1 mm path length. Solutions of BCS were prepared as described in prior sections. Emulsions were then prepared with the addition of deuterated dodecane. The raw SANS data were processed with wavelength-dependent correction to the incident spectrum, detector efficiency, and sample transmission.^[34] The data were absolutely scaled, giving scattering intensity $I(Q)$ as a function of Q , using the scattering from a standard sample (a solid blend of protiated and perdeuterated polystyrene) based

on established methods.^[35] All samples were confirmed to be free of multiple scattering. SANS data were fitted using SASView 4.2.2.^[36] Scattering length densities (SLDs) were calculated from the monomer using the Neutron activation and scattering calculator website from the NIST Centre for Neutron Research.^[30]

Transmission Electron Microscopy (TEM) of BCS Solutions: TEM of BCS solutions was conducted using a Tecnai G2 Spirit Twin microscope (FEI, Czech Republic). To prepare the specimens for TEM, a 4 μL sample solution was dropped onto a 300-mesh copper TEM grid coated with a thin, electron-transparent carbon film. The excess solution was then removed after 15 min of sedimentation using the “fast drying method” to minimize oversaturation during the drying process. The particles were negatively stained with a 2 wt.% solution of uranyl acetate, which was dropped onto the dried nanoparticles and left for 15 sec before being removed in the same manner as the previous solution. The sample was then left to dry completely and observed using the TEM microscope.

To observe the sample morphology at elevated temperatures, specimens were prepared using a similar method but with an electric oven heated to 40 °C. The solutions and all tools for sample preparation, including grids, tweezers, and uranyl acetate solutions, were incubated in the oven before being deposited onto the TEM grid and left to sediment for 15 min at 40 °C. The excess solution was then removed, and the particles were negatively stained with preheated solution of uranyl acetate and left to dry completely at 40 °C. This approach allowed for the stabilization of the sample morphology at elevated temperatures, which could then be observed using the TEM microscope at laboratory temperature, as documented in previous studies.^[37,38]

Hot-Stage Light Microscopy of Emulsions: The emulsions were subjected to hot stage light microscopy, with the use of a Nikon Eclipse 80i microscope with a Linkam THMS600 temperature control stage (UK). To begin, a small quantity of the emulsion (which was kept in the refrigerator at 4 °C before the experiment) was placed on a microscope cover glass, followed by another cover glass, and then inserted into the temperature control stage. The initial temperature of the stage was set to 5 °C. The sample was left to equilibrate for 5 min and a micrograph was recorded. Then the temperature was gradually raised (heating rate 1°C min⁻¹) until it reached 10 °C, where it was kept for another 5 min, and an LM micrograph was captured. This process was repeated for temperatures of 10, 15, 20, 25, and 30 °C.

Supporting Information

Supporting Information is available from the Wiley Online Library or from the author.

Acknowledgements

The EPSRC is thanked for funding the research (EP/T00813X/1). The grant is also supported by equipment funded by the Royal Society Research Grant (RF17-9915). Dr Daniel Lester at the Warwick Polymer Characterisation RTP is thanked for gel-permeation chromatography on the BCS samples. The authors gratefully acknowledge the Science and Technology Facilities Council (STFC) for access to neutron beamtime at ISIS, and for the provision of sample preparation facilities (experiment 2220037).

Conflict of Interest

The authors declare no conflict of interest.

Data Availability Statement

The data that support the findings of this study are available from the corresponding author upon reasonable request

Keywords

colloids, emulgels, lower critical solution temperature, neutron scattering, radical polymerisation

Received: September 8, 2023

Revised: October 4, 2023

Published online:

- [1] J. V. M. Weaver, S. P. Rannard, A. I. Cooper, *Angew. Chemie – Int. Ed.* **2009**, *48*, 2131.
- [2] R. T. Woodward, L. Chen, D. J. Adams, J. V. M. Weaver, *J. Mater. Chem.* **2010**, *20*, 5228.
- [3] M. A. Da Silva, A. Rajbanshi, D. Opoku-Achampong, N. Mahmoudi, L. Porcar, P. Gutfreund, A. Tummino, A. Maestro, C. A. Dreiss, M. T. Cook, *Macromol. Mater. Eng.* **2022**, *307*, 2200321.
- [4] A. Rajbanshi, M. A. Da Silva, D. Murnane, L. Porcar, C. A. Dreiss, M. T. Cook, *Polym. Chem.* **2022**, *13*, 5730.
- [5] R. T. Woodward, R. A. Slater, S. Higgins, S. P. Rannard, A. I. Cooper, B. J. L. Royles, P. H. Findlay, J. V. M. Weaver, *Chem. Commun.* **2009**, 3554.
- [6] A. Y. C. Koh, B. R. Saunders, *Chem. Commun.* **2000**, *6*, 2461.
- [7] R. Baudry, D. C. Sherrington, *Macromolecules* **2006**, *39*, 1455.
- [8] R. T. Woodward, J. V. M. Weaver, *Polym. Chem.* **2011**, *2*, 403.
- [9] C. M. Caramella, S. Rossi, F. Ferrari, M. C. Bonferoni, G. Sandri, *Adv. Drug Delivery Rev.* **2015**, *92*, 39.
- [10] P. Kan, X.-Z. Lin, M.-F. Hsieh, K.-Y. Chang, *J. Biomed. Mater. Res. – Part B Appl. Biomater.* **2005**, *75*, 185.
- [11] Y. C. Kim, M. D. Shin, S. F. Hackett, H. T. Hsueh, R. Lima E Silva, A. Date, H. Han, B.-J. Kim, A. Xiao, Y. Kim, L. Ogunnaik, N. M. Anders, A. Hemingway, P. He, A. S. Jun, P. J. McDonnell, C. Eberhart, I. Pitha, D. J. Zack, P. A. Campochiaro, J. Hanes, L. M. Ensign, *Nat. Biomed. Eng.* **2020**, *4*, 1053.
- [12] C. Ni, Y. Wang, Q. Hou, X. Li, Y. Zhang, Y. Wang, Y. Xu, Y. Zhao, *J. Pet. Sci. Eng.* **2020**, *193*, 107410.
- [13] P. Raffa, A. A. Broekhuis, F. Picchioni, *J. Pet. Sci. Eng.* **2016**.
- [14] J.-F. Lutz, *Adv. Mater.* **2011**, *23*, 2237.
- [15] J.-F. Lutz, Ö. Akdemir, A. Hoth, *J. Am. Chem. Soc.* **2006**, *128*, 13046.
- [16] J.-F. Lutz, *J. Polym. Sci. Part A Polym. Chem.* **2008**, *46*, 3459.
- [17] J.-F. Lutz, A. Hoth, K. Schade, *Des. Monomers Polym.* **2009**, *12*, 343.
- [18] M. T. Cook, P. Haddow, S. B. Kirton, W. J. Mcauley, *Adv. Funct. Mater.* **2021**, *31*, 2008123.
- [19] M. A. Da Silva, I. A. Farhat, E. P. G. Arêas, J. R. Mitchell, *Biopolymers* **2006**, *83*, 443.
- [20] Q. Li, L. Wang, F. Chen, A. P. Constantinou, T. K. Georgiou, *Polym. Chem.* **2022**, *13*, 2506.
- [21] M. A. Ward, T. K. Georgiou, *Polym. Chem.* **2013**, *4*, 1893.
- [22] N. Badi, *Prog. Polym. Sci.* **2017**, *66*, 54.
- [23] S.-I. Yamamoto, J. Pietrasik, K. Matyjaszewski, *J. Polym. Sci. Part A Polym. Chem.* **2008**, *46*, 194.
- [24] N. Badi, *Prog. Polym. Sci.* **2017**, *66*, 54.
- [25] A. P. Constantinou, L. Wang, S. Wang, T. K. Georgiou, *Polym. Chem.* **2022**, *14*, 223.
- [26] A. A. A. Smith, C. L. Maikawa, H. Lopez Hernandez, E. A. Appel, *Polym. Chem.* **2021**, *12*, 1918.
- [27] D. G. Lessard, M. Ousalem, X. X. Zhu, A. Eisenberg, P. J. Carreau, *J. Polym. Sci. Part B Polym. Phys.* **2003**, *41*, 1627.
- [28] L. Yu, J. Ding, *Chem. Soc. Rev.* **2008**, *37*, 1473.
- [29] R. T. Woodward, R. A. Slater, S. Higgins, S. P. Rannard, A. I. Cooper, B. J. L. Royles, P. H. Findlay, J. V. M. Weaver, *Chem. Commun.* **2009**, *24*, 3554.

- [30] NIST SLD Calculator, <https://www.ncnr.nist.gov/resources/sldcalc.html> (accessed: April 2021).
- [31] R. Pelton, *J. Colloid Interface Sci.* **2010**, *348*, 673.
- [32] A. Blanazs, S. P. Armes, A. J. Ryan, *Macromol. Rapid Commun.* **2009**, *30*, 267.
- [33] B. Hammouda, D. L. Ho, S. Kline, *Macromolecules* **2004**, *37*, 6932.
- [34] R. K. Heenan, J. Penfold, S. M. King, *J. Appl. Crystallogr.* **1997**, *30*, 1140.
- [35] G. D. Wignall, F. S. Bates, *J. Appl. Crystallogr.* **1987**, *20*, 28.
- [36] SasView version 4.2.2, <https://www.sasview.org/2019-05-20-release-4.2.2/> (accessed: January 2023)
- [37] K. Kolouchova, O. Groborz, M. Slouf, V. Herynek, L. Parmentier, D. Babuka, Z. Cernochova, F. Koucky, O. Sedlacek, M. Hruby, R. Hoogenboom, S. Van Vlierberghe, *Chem. Mater.* **2022**, *34*, 10902.
- [38] J. Skvarla, J. Zedník, M. Slouf, S. Pispas, M. Stepánek, *Eur. Polym. J.* **2014**, *61*, 124.